International Journal of
Applied Mathematics,
Electronics and Computers
IJAMEC
ISSN:2147-8228 www.atscience.org/IJAMEC
Advanced Technology and Science
Original Research Paper

H_2, H_∞ and H_2/H_∞ Control of Elastic Beam Vibrations Using Piezoelectric Actuator

Fevzi Cakmak Bolat[1], Selim Sivrioğlu*[2]

Accepted : 25/09/2017 Published: 30/09/2017 **DOI: 10.18100/ijamec.2017331880**

Abstract: In this research study, vibration of an elastic cantilever beam is suppressed with norm based controllers by using the piezoelectric actuator. Beam like distributed parameter structures have theoretically infinite number of vibration modes and uncontrolled high frequency vibration modes in a control application may be excited by the controller due to spillover effect. In this paper, H_2, H_∞ and mixed norm objective H_2/H_∞ controllers are designed by introducing a multiplicative uncertainty which represents unmodeled high-frequency dynamics in the control system. The designed controllers are realized in experiments and performances of the controllers are compared using frequency and time domain responses.

Keywords: *Robust control, elastic beam vibrations, active vibrations control, piezoelectric actuator*

1. Introduction

Many research works have been carried out especially in aerospace structures to create active and semi-active control systems by embedding piezoelectric materials into structures. Such structures are called smart or adaptive structures, and control applications are important for these systems [1-6]. Piezoelectric materials have important characteristics to create smart structures [7]. When an electric field is applied to a piezoelectric material, it is deformed therefore it is suitable to use as an actuator in control systems. Furthermore, the piezoelectric material generates voltage when it is deformed and it can be used as a sensor to detect deformations. Distributed parameter structures with piezoelectric layers may have great potentials to create adaptive structures for responding on changing external conditions.

Robustness of a structural control system may sometimes be an issue due to the disturbance effect of high order structural modes [8]. Modal behaviors of distributed parameter systems such as beams, shafts, plates should be considered especially in control design applications. In these systems, there are theoretically infinite number of modal frequencies and in practical control applications the uncontrolled modes may be excited by the controller. This phenomenon is called spillover effect and may be danger if any measures is not taken.

Norm based linear control approaches have been studied in the control of engineering systems in recent years due to some distinct advantages [9-10]. In general, different control specifications should be satisfied in a control system. Considering norm based controllers, while H_∞ control mainly enforces the robust stability, H_2 control improves the transient behavior of the control system. The multi-objective H_2/H_∞ control combines both design objectives. It is an advantage that both frequency and time domain specifications are performed in vibration control of the distributed parameter systems.

This paper begins with the modeling of the cantilever beam for control design. Also, a modal analysis is realized and natural frequencies of the beam are obtained using different methods. Norm based controller designs are presented and the controller and closed loop frequency responses are shown for each control case in simulations. The experimental setup is introduced in detail. The experimental results are presented in frequency and time domain for each control. Finally, the control performances are compared using frequency responses.

2. Modeling of the cantilever beam

The cantilever beam with an attached piezoelectric actuator is schematically shown in Figure 1(a). Here x coordinate is related with the longitudinal dynamics and y coordinate shows the direction of vibration of the beam. The force that piezoelectric patch generated is shown by f and applied to the beam at the distance x_f . The distance x_s denotes the sensor location. For each vibration mode, the separated equation of motion is given by

$$\ddot{x}_n(t) + 2\varsigma\omega_n\dot{x}_n(t) + \omega_n^2 x_n(t) = f(t)\psi_n(x_f) \tag{1}$$

where ω_n is the mode natural frequency, ς is the damping coefficient and $\psi_n(\cdot)$ is the mode shape function. The state space equation for each modal behavior is obtained using equation (1) as follows

$$\dot{x}(t) = A_n x(t) + B_n u(t) \tag{2}$$

where $x(t)$ is the state vector, A_n is the system matrix, B_n is the control input matrix and $u(t)$ is the control input. The structure of the state vector and matrices are as follows

1Mechanical Engineering Department Gebze Technical University, Gebze 41400 – Kocaeli/Turkey
2 Mechanical Engineering Department Gebze Technical University, Gebze 41400 – Kocaeli/Turkey
Corresponding Author:Email: fcbolat@gtu.edu.tr

$$x=\begin{bmatrix} x_n(t) \\ \dot{x}_n(t) \end{bmatrix},\quad A_n=\begin{bmatrix} 0 & 1 \\ -\omega_n^2 & -2\varsigma\omega_n \end{bmatrix},\quad B_n=\begin{bmatrix} 0 \\ \psi_n(x_f) \end{bmatrix} \tag{3}$$

In distributed systems, the displacement measured by the sensor is modeled as the multiplication of the modal displacement with the mode shape function at the considered point. For the sensor location, the output is written as

$$y(x,t)=\sum_{n=1}^{\infty} x_n(t)\psi_n(x_s) \tag{4}$$

Using equation (4) for each vibration mode the output of the state space equation is obtained as

$$y=C\,x_n(t)=[C_n \quad 0\,]x_n(t) \tag{5}$$

where the matrix C_n is computed using the following mode shape function.

$$C_n=\psi_n(x_s)=\sinh\beta_n x_s-\sin\beta_n x_s -\left[\frac{\sinh\beta_n L_b+\sin\beta_n L_b}{\cosh\beta_n L_b+\cos\beta_n L_b}\right](\cosh\beta_n x_s-\cos\beta_n x_s) \tag{6}$$

where

$$\beta_n=\left(\omega_n\sqrt{\frac{\rho A}{EI}}\right)^{1/2}=\left(\frac{2n-1}{2}\pi+e_n\right)\frac{1}{L} \tag{7}$$

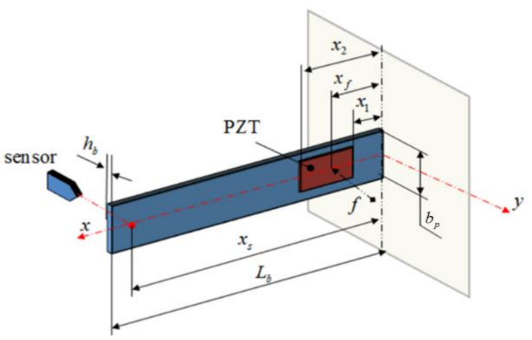

(a)

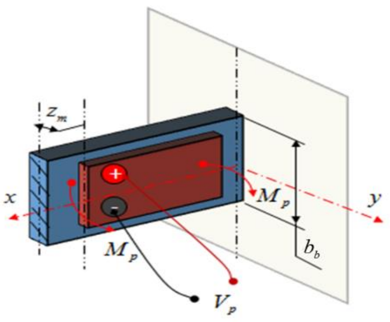

(b)

Fig. 1. Beam structure for modeling (a) cantilever beam (b) PZT layc

Table .1 Parameters of the cantilever beam and PZT patch

Symbol	Meaning	Value	Unit
L_b	Length of the beam	0.35	m
b_b	Width of the beam	0.040	m
h_b	Thickness of the beam	0.001	m
ρ_b	Density of the beam	2780	kg/m^3
E_b	Young's modulus of the beam	70	GPa
L_p	Length of the PZT patch	0.050	m
b_p	Width of the PZT patch	0.030	m
h_p	Thickness of the PZT patch	0.0005	m
d_{31}	Piezoelectric charge constant	-1.8×10^{-10}	C/N
ρ_p	Density of the PZT patch	7800	kg/m^3
E_p	Young's modulus of the PZT patch	6.2	GPA
x_f	Location of the PZT	0.080	m

The bending moment generated by the PZT patch attached on the beam shown schematically in Figure 1(b) is defined as

$$M_p=-e_{31}V_p b_p z_m \tag{8}$$

where V_p is the applied voltage, z_m is the distance from the half thickness of the beam to the half thickness of the PZT. In addition, b_p shows the width of the PZT and e_{31} shows the PZT patch constant. The force applied by PZT actuator given in equation (1) is derived as follows.

$$f(t)=\frac{M_p(t)}{l_i}\left[\psi_n'\left(\frac{x_1+x_2}{2}\right)\right]=\frac{-d_{31}E_p b_p\left(\frac{h_b}{2}+\frac{h_p}{2}\right)V_p}{\rho_b A_b L_b^3+\rho_p A_p L_p^3}\left[\psi_n'\left(\frac{x_1+x_2}{2}\right)\right] \tag{9}$$

If the modeling is extended for n modes, the state space structure is obtained as follows.

$$\frac{d}{dt}\begin{bmatrix} x_1 \\ x_2 \\ \vdots \\ x_n \end{bmatrix}=\begin{bmatrix} A_1 & & & 0 \\ & A_2 & & \\ & & \ddots & \\ 0 & & & A_n \end{bmatrix}\begin{bmatrix} x_1 \\ x_2 \\ \vdots \\ x_n \end{bmatrix}+\begin{bmatrix} B_1 \\ B_2 \\ \vdots \\ B_n \end{bmatrix}u$$
$$y=[C_1 \quad C_2 \quad \dots \quad C_n]\begin{bmatrix} x_1 \\ x_2 \\ \vdots \\ x_n \end{bmatrix} \tag{10}$$

The mode shapes of the cantilever beam with normalized dimensions and modal displacements are obtained as shown in Figure 2. The locations of the displacement sensor and PZT patch are depicted in the figure to understand whether the nodal points occur at these points. As seen in Figure 2, the nodal points are different locations from the sensor and PZT locations for the first four vibration modes.

Distributed systems have theoretically infinite number of vibration modes. The state space model obtained in equation (10) considers certain number of modes. In this study, the full order model of the cantilever beam is built by considering the vibration modes up to 1 kHz. In practice the modal contributions of the higher order modes are inconsiderable due to small modal amplitudes. Also, the reduced order model which contains the first two modes up to 40 Hz are used for controller designs. The frequency responses of the full and reduced order models are shown in Figure 3.

Natural frequencies of the cantilever beam at each vibration modes are obtained using different approaches and the frequency values are given in Table 2. The state space model used for control designs is derived using the analytical model as given above. In the analytical model, PZT patch is not considered in the modeling. Modal frequencies obtained in experiments are different from the analytical model results due to the PZT patch attached on the beam surface. The FEM model results clearly verify the PZT patch effect.

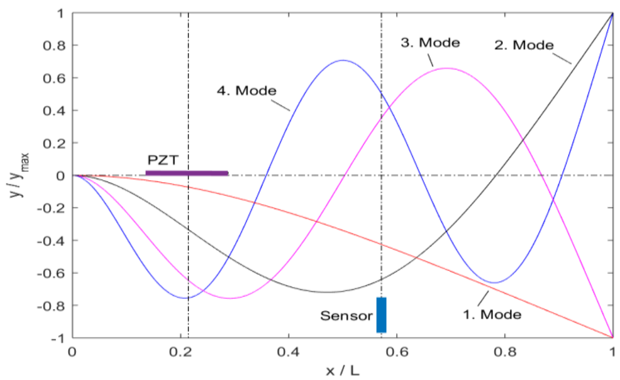

Fig. 2. Mode shapes of the cantilever beam

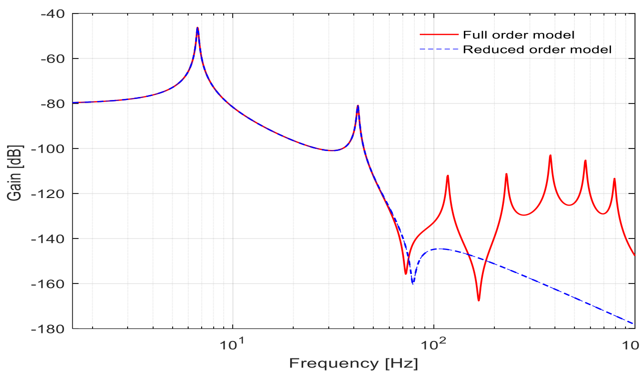

Fig. 3. Frequency response of the beam model

Table.2 Natural frequencies of the beam vibration modes

Mode Number	Analytical Model [Hz]	FEM Model (ANSYS) [Hz]		Experimental results [Hz]
	without PZT	without PZT	with PZT	with PZT
1	6.67	6.78	6.60	5.50
2	41.84	41.51	38.20	33.00
3	117.15	114.67	96.61	98.50
4	229.57	233.91	212.00	212.50

3. Norm Based Control Designs

3.1. H_∞ Control

In distributed parameter control systems such as beams, rotors and plates, unmodeled high frequency dynamics may be excited by the designed controller. This phenomenon is called spillover effect and it should be considered in the controller design. Since H_∞ control theory essentially considers such unstructured uncertainties in the control design it is very suitable for this type of control structures to avoid spillover.

The H_∞ control design structure is shown in Figure 4. In this block representation $P_r(s)$ and $K(s)$ show the reduced order system model and the controller to be designed, respectively. Also, $G(s)$ is the generalized or augmented system. The design filters $W_1(s)$ and $W_2(s)$ are used for the robust performance and the robust stability of the closed loop system. η and ε are scalar weights for the system disturbance and sensor noise and are taken as $\eta = 1$, $\varepsilon = 0.01$. The transfer matrix from the system disturbance d and sensor noise n to the controlled outputs z_1 and z_2 is obtained as

$$\begin{bmatrix} z_1 \\ z_2 \end{bmatrix} = \begin{bmatrix} W_1(s)P_r(s)S(s)\eta & W_1(s)T(s)\varepsilon \\ W_2(s)T(s)\eta & W_2(s)T_a(s)\varepsilon \end{bmatrix} \begin{bmatrix} d \\ n \end{bmatrix} \tag{11}$$

$$z = G_{zw}(s)w$$

Here, $G_{zw}(s)$ includes all transfer functions from w to z. The transfer functions are given as $T(s) = K(s)(I - P_r(s)K(s))^{-1}P_r(s)$ $S(s) = (I - P_r(s)K(s))^{-1}$, and $T_a(s) = K(s)(I - P_r(s)K(s))^{-1}$. The H_∞ control design objective is to obtain a controller that minimize infinity norm of the closed loop transfer matrix such as [11]

$$\left\| G_{zw}(s) \right\|_\infty < \gamma \tag{12}$$

where $\gamma > 0$. The control system performance strongly depends on the frequency shaping filters. The filters $W_1(s)$ and $W_2(s)$ are selected as

$$W_1 = p_1 \times \frac{\sigma}{s + \omega_1}, \quad W_2 = p_2 \times \frac{s^2 + 2\omega_{nm}\varsigma_{nm} + \omega_{nm}{}^2}{s^2 + 2\omega_{dm}\varsigma_{dm} + \omega_{dm}{}^2} \tag{13}$$

The robust stability filter $W_2(s)$ is determined by using neglected high frequency dynamics. For this aim, while the filter nominator frequency ω_{nm} is taken as the controlled last vibration mode frequency or the second mode frequency, the denominator frequency ω_{dm} is selected as the first unmodeled frequency or the third vibration mode frequency. The multiplicative uncertainty $\Delta_m(j\omega)$ in the system is obtained as

$$\Delta_m(j\omega) = \frac{P_f(j\omega) - P_r(j\omega)}{P_r(j\omega)} \tag{14}$$

where $P_f(j\omega)$ shows the full order system model. The robust stability filter $W_2(s)$ essentially covers the unstructured uncertainties existing in the system such as

$$\left| \Delta_m(j\omega) \right| \le \left| W_2(j\omega) \right| \qquad \forall \omega \tag{15}$$

Frequency responses of the multiplicative uncertainty and robust stability filter are shown in Figure 5. Using the augmented system model obtained using the control design structure the H_∞ controller is computed as

$$\begin{aligned} \dot{x}_{K\infty} &= A_{K\infty}x_{K\infty} + B_{K\infty}y \\ u &= C_{K\infty}x_{K\infty} + D_{K\infty}y \end{aligned} \tag{16}$$

The frequency response of the H∞ controller is shown in Figure 6. Using the designed H∞ controller, the closed loop system of the full order system is obtained and the frequency response is presented in Figure 7. The targeted first and second modes are suppressed perfectly while the other uncontrolled modes are not excited by the controller.

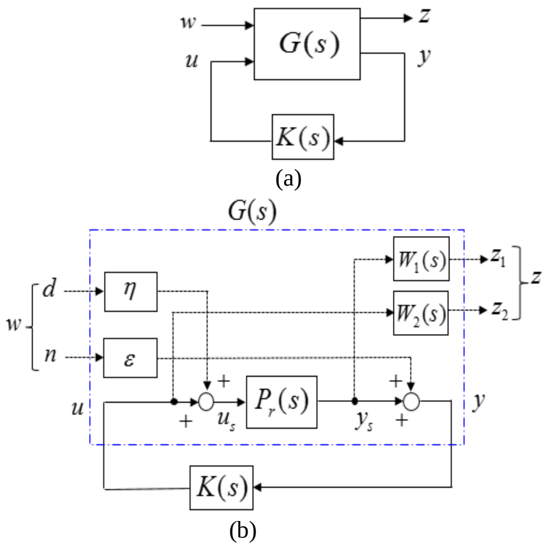

Fig. 4. H_∞ control design structure (a) Generalized plant (b) block structure

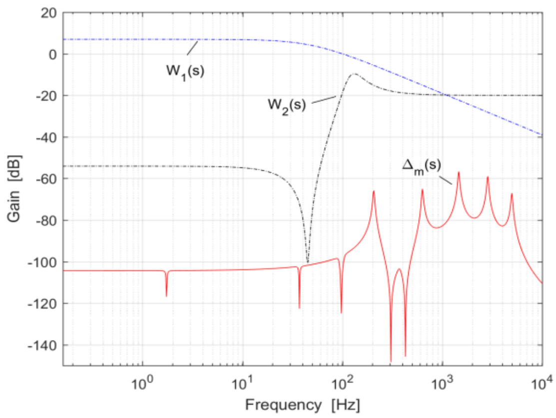

Fig. 5. Frequency response of multiplicative uncertainty and W_1 and W_2 filters

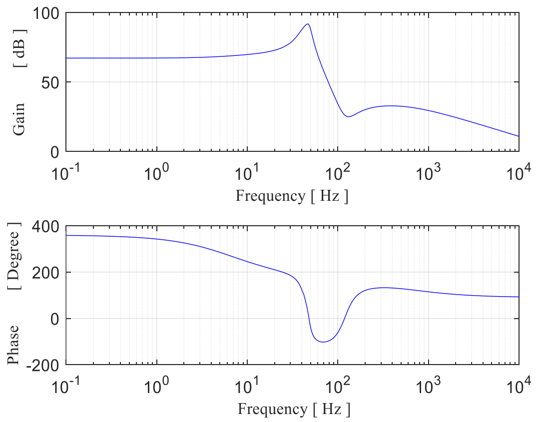

Fig. 6. Frequency response of the H_∞ controller

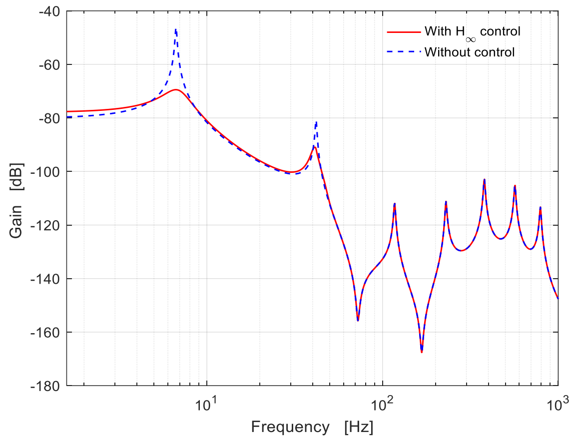

Fig. 7. Close loop frequency response with H_∞ controller

3.2. H_2 Control

Control design specifications in a control system such as noise attenuation or regulation against random disturbances are more essentially handled in H_2 or LQG control. The time response and transient behavior of the feedback control system can be improved with H_2 control. In H_2 control, the input v is a white noise disturbance with unit covariance.

The H_2 control design block structure is shown in Figure 8. In this control block, W_3 and W_4 are the system disturbance spectrum and sensor noise spectrum respectively. The design filters $W_1(s)$ and $W_2(s)$ are the same with the H_∞ control design.

$$\begin{bmatrix} z_1 \\ z_2 \end{bmatrix} = \begin{bmatrix} W_1(s)S(s)W_3 & W_1(s)T(s)W_4 \\ W_2(s)T_a(s)W_3 & W_2(s)T_a(s)W_4 \end{bmatrix} \begin{bmatrix} v_1 \\ v_2 \end{bmatrix}$$

$$z = T_{zv}(s)v \tag{17}$$

$T_{zv}(s)$ shows the transfer matrix from v to z. The control design objective is to minimize H_2 norm of the closed loop transfer matrix such as

$$\|T_{zv}(s)\|_2 < \nu \tag{18}$$

where $\nu > 0$. The H_2 controller is computed as

$$\begin{aligned} \dot{x}_{K2} &= A_{K2}x_{K2} + B_{K2}y \\ u &= C_{K2}x_{K2} + D_{K2}y \end{aligned} \tag{19}$$

The H_2 controller frequency response is illustrated in Figure 9. The closed loop frequency response of the system with H_2 controller is shown in Figure 10. The first and second vibration modes are suppressed and the other modes are not effected anymore.

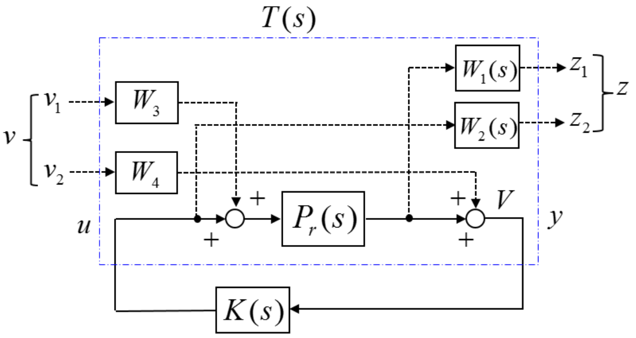

Fig. 8. Block diagram of H_2 control design

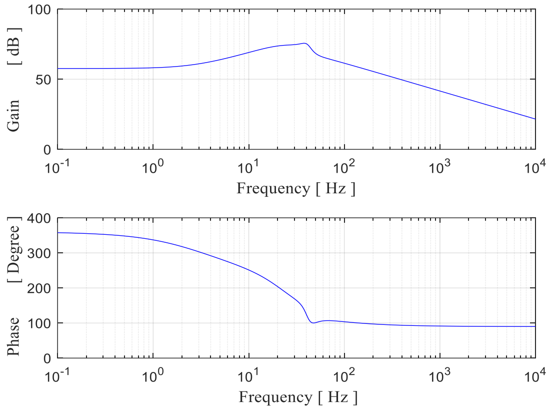

Fig. 9. Frequency response of H_2 controller

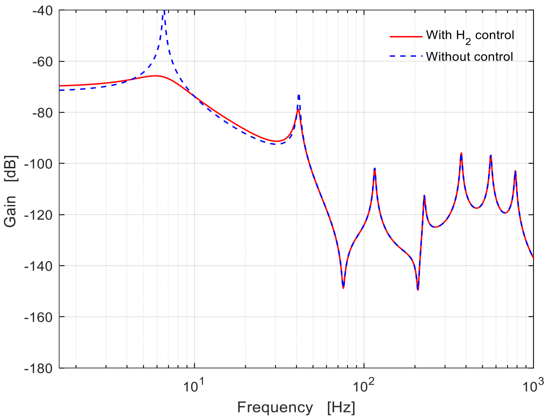

Fig. 10. Close loop frequency responce with H_2 controller

3.3. Mixed H_2/H_∞ Control

All design specifications in a control system are not captured by an H_∞ or H_2 controller. While H_∞ control mainly enforces the closed-loop stability, H_2 control improves the transient behavior of the control system. A multi-objective control that combines both design objectives is highly desirable in practice.

The generalized plant structure of the multi-objective control is shown in Figure 11. The output channel z_∞ is associated with the H_∞ performance while the channel z_2 is associated with the H_2 performance. Also, $T_\infty(s)$ and $T_2(s)$ are the closed-loop transfer functions from w to z_∞ and z_2, respectively. The state-space realization of the plant is given by

$$\begin{aligned} \dot{x} &= Ax + B_1 w + B_2 u \\ z_\infty &= C_\infty x + D_{\infty 1} w + D_{\infty 2} u \\ z_2 &= C_2 x + D_{21} w + D_{22} u \\ y &= C_y x + D_{y1} w \end{aligned} \tag{20}$$

Using the closed loop transfer functions, minimization of a trade-off criterion can be formed such that design a controller K(s) that minimizes the mixed H_2/H_∞ norm criterion

$$\alpha \|T_\infty(s)\|_\infty^2 + \beta \|T_2(s)\|_2^2 \qquad \alpha, \beta \geq 0 \tag{21}$$

subject to

$$\|T_\infty(s)\|_\infty < \gamma_0, \quad \|T_2(s)\|_2 < \nu_0, \qquad \gamma_0, \nu_0 > 0 \tag{22}$$

The mixed H_2/H_∞ controller is obtained as follows

$$\begin{aligned} \dot{x}_{K2\infty} &= A_{K2\infty} x_{K2\infty} + B_{K2\infty} y \\ u &= C_{K2\infty} x_{K2\infty} + D_{K2\infty} y \end{aligned} \tag{23}$$

The frequency response of the H_2/H_∞ controller is given in Figure 12. The closed loop control system frequency response with the mixed H_2/H_∞ controller is depicted in Figure 13.

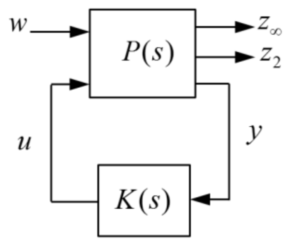

Fig. 11. Multi-objective control structure

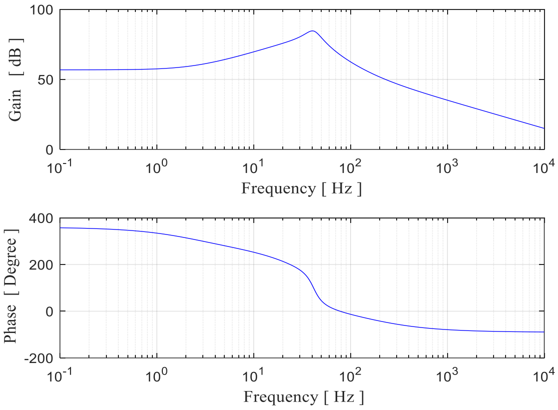

Fig. 12. Frequency response of H_2/H_∞ controller

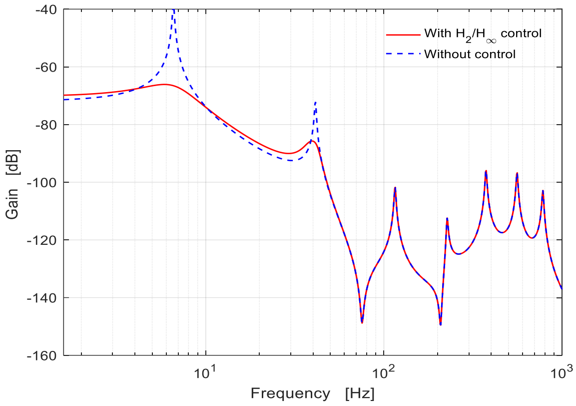

Fig. 13. Close loop frequency response with H_2 / H_∞ controller

4. Experimental System

The photo of the experimental system setup is shown in Figure 14. An elastic $(L_p \times b_p \times h_p) = 350 \times 40 \times 1$ mm dimension aluminum beam with attached PZT actuator is fixed at one end using a clamp. In the experimental system, a PI DuraAct (P-876.A12) PZT patch with $61 \times 35 \times 0.5$ mm dimension is installed. Supply voltage for the PZT patch is between -100 $+400$ V. Power supplies, optic sensor, driver(E-413.D2) for piezoelectric actuator and Quanser-Q8 unit are used as peripheral devices. Vibration analysis of the beam is performed with a Bruel&Kjaer 3053 device. The designed controllers are realized using dSpace 1104 control card. The controllers are discretized and compiled in the state space form using a Matlab/Simulink file and installed on dSpace control card.

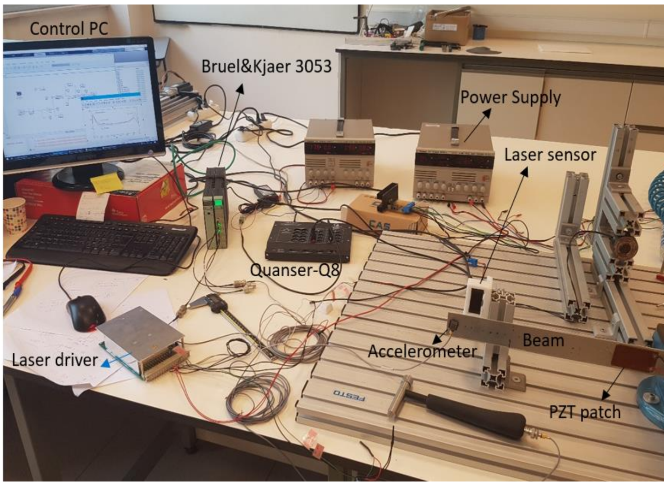

Fig. 14. Experimental system

4.1. Experimental Results

The closed loop frequency responses of the beam obtained in experiments with H_∞, H_2 and H_2 / H_∞ controllers are shown in Figure 15, respectively. Since the first two modes of the cantilever beam are targeted in control design, these modes are suppressed by the controllers in different levels. In these results, the uncontrolled modes are not excited by the controllers. The time history responses of the beam displacements at sensor location are shown in Figure 16 for designed controllers. The time response of the control system with H_2 control is comparatively better than the other controllers. The time history responses of the control inputs for every control are shown in Figure 17. The largest control input especially at the initial state is produced by H_∞ control. This result reflects the H_∞ control characteristics. The amplitude of the control input produced by the H_2 / H_∞ control is almost half of the other controller inputs (Figure 17(c)). The frequency responses of the closed loop system with norm based controllers are compared in Figure 18.

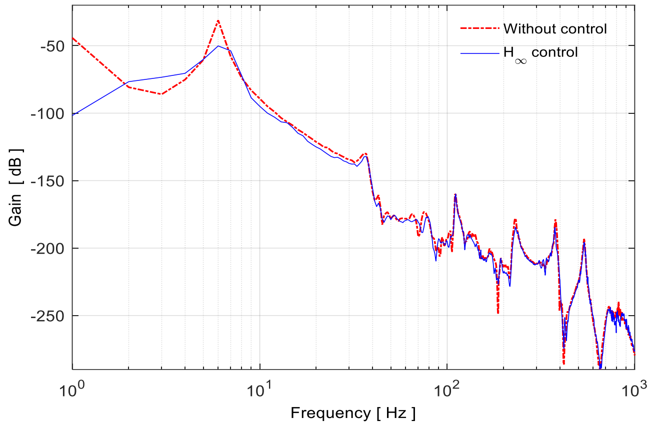

(a) H_∞ control

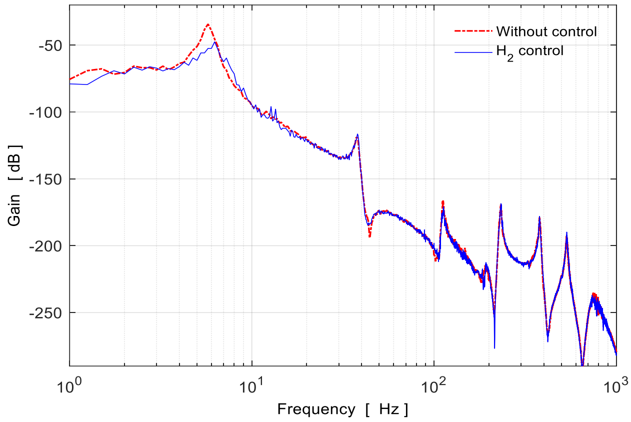

(b) H_2 control

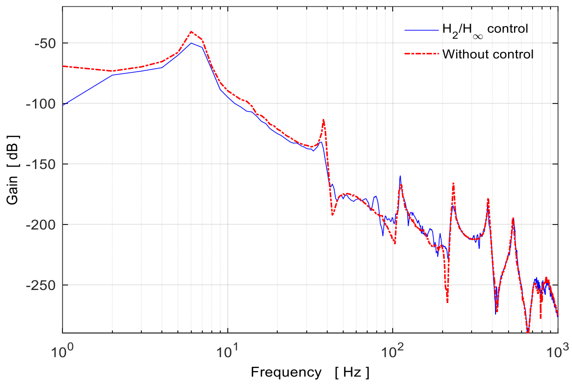

(c) H_2 / H_∞ control

Fig. 15. Experimental closed loop frequency response

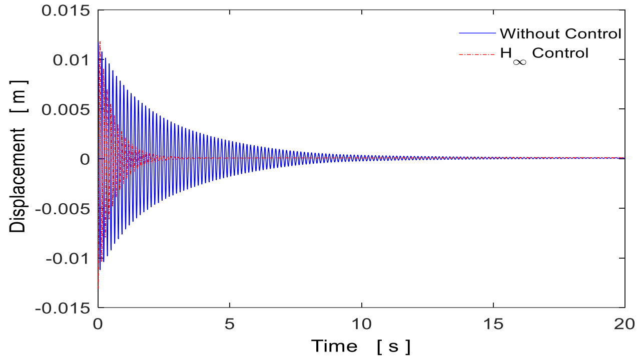

(a) H_∞ control

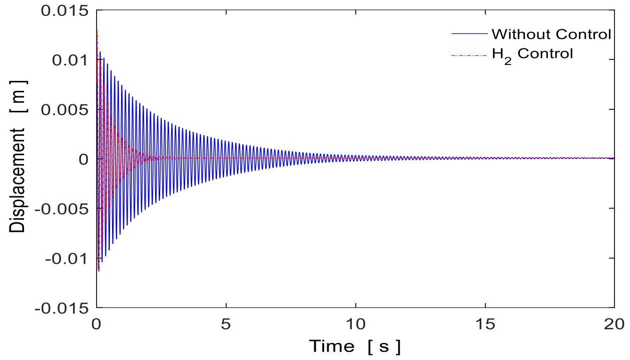

(b) H_2 control

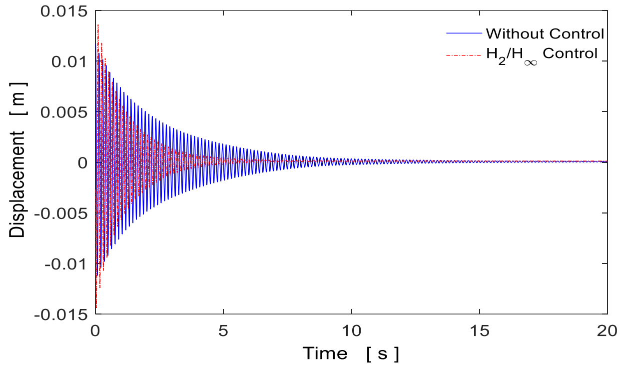

(c) H_2 / H_∞ control

Fig. 16. Time history responses of the displacements

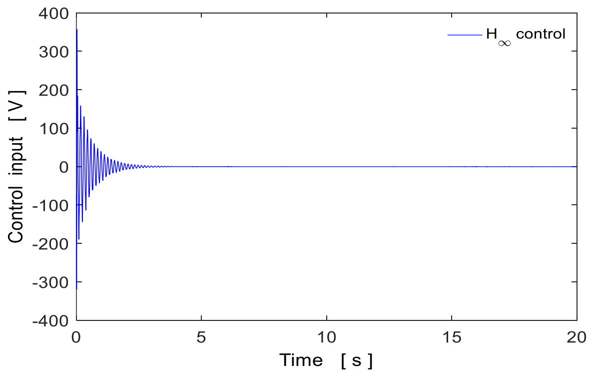

(a) H_∞ control

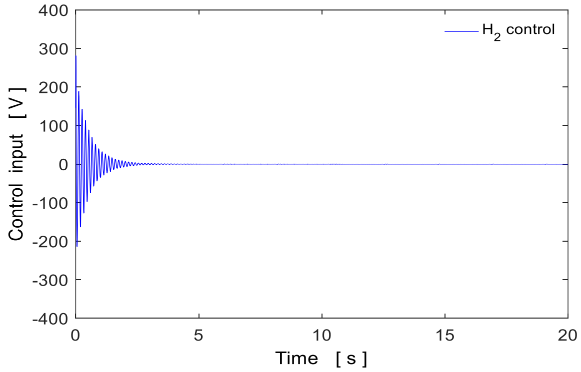

(b) H_2 control

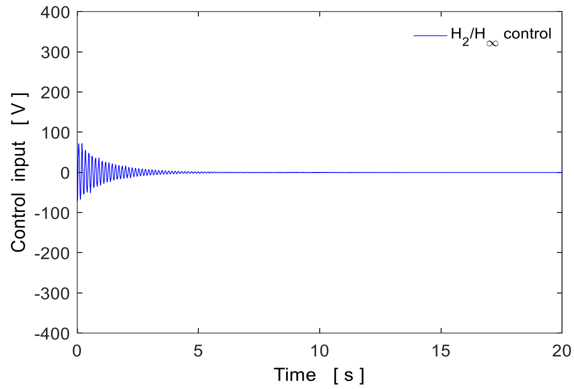

(c) H_2 / H_∞ control

Fig. 17. Time history responses of the control inputs

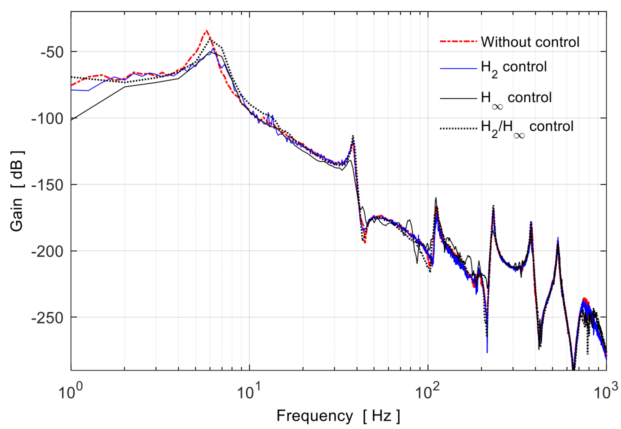

Fig. 18. Comparison of the experimental closed loop frequency responses.

4.2 Robustness test

Since norm based control design approaches consider uncertainty in the control system design, a robustness test can be realized experimentally. To understand the robustness of the designed controllers, a tip mass having %10 percent of the total mass is attached to the cantilever beam. For every designed controller, the closed loop time history responses of the displacements with tip mass are shown in Fig. 19 and Fig.20. Also, the control input voltages are given in Fig.21. Although some increase in the magnitude of the displacement is observed, the controllers suppress the vibration of the beam effectively.

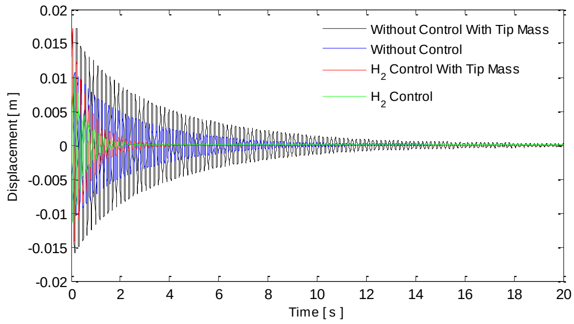

(a) H_2 control

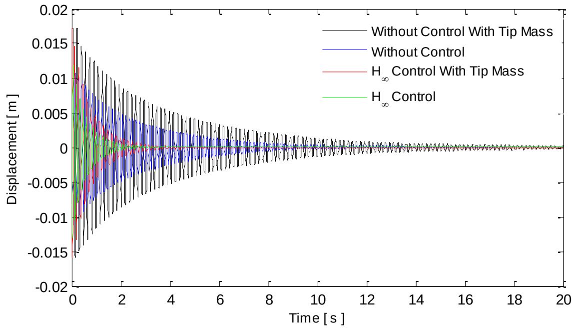

(b) H_∞ control

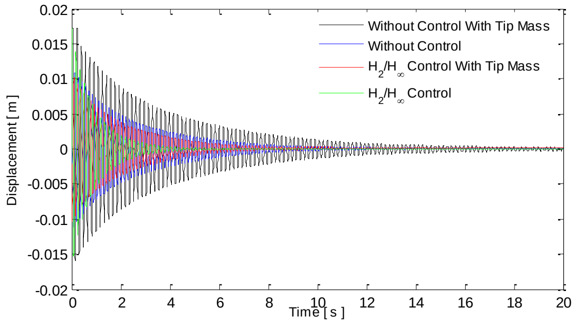

(c) H_2 / H_∞ control

Fig. 19. Time history responses of the displacements with tip mass

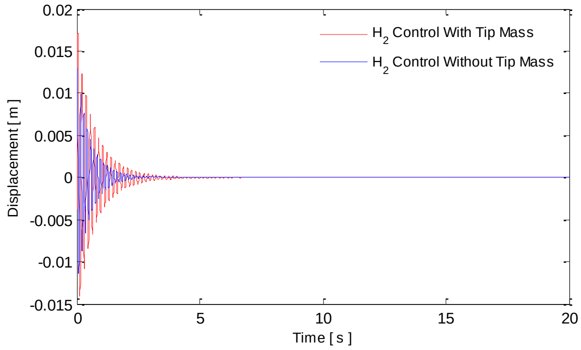

(a) H_2 control

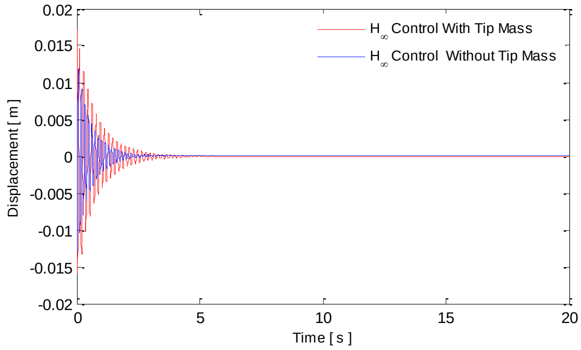

(b) H_∞ control

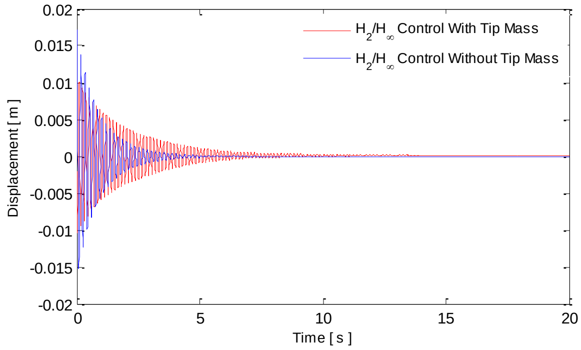

(c) H_2 / H_∞ control

Fig. 20. Comparison time history responses of the displacements with tip mass

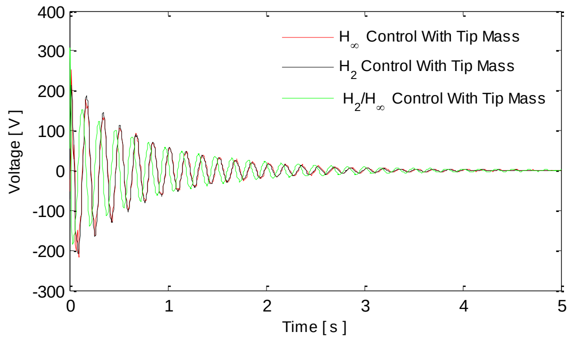

Fig. 21. Comparison time history responses of the control inputs

5. Conclusion

Vibration suppression of the flexible cantilever beam with a piezoelectric actuator is investigated using norm based H_2, H_∞ and H_2 / H_∞ controllers. Neglected or unmodeled high-frequency dynamics in the beam control system are covered with robust stability filters in the control design to avoid the spillover effect. The experiments are realized for every control to understand the robustness and performance improvements in the control system. The frequency responses and time history responses are presented for each control case. The targeted vibration modes are suppressed by the proposed controllers in different levels.

References

[1] Stavroulakisa GE, Foutsitzic G, Hadjigeorgiouc E, Marinovad D, Baniotopoulose C.C (2005) Design and robust optimal control of smart beams with application on vibrations suppression. Advances in Engineering Software Volume 36 Issue 11-12: 806–813

[2] Fei J. (2005) Active Vibration Control of Flexible Steel Cantilever Beam Using Piezoelectric Actuators. IEEE DOI: 10.1109/SSST.2005.1460873

[3] Kai Z, Scorletti G, Ichchou M, Mieyeville F (2013) Robust active vibration control of piezoelectric flexible structures using deterministic and probabilistic analysis. Journal of Intelligent Material Systems and Structures Vol 25(6) 665-679. DOI: 10.1177/1045389X13500574

[4] M Sahin, Karadal FM, Yaman Y, Kircali OF, Nalbantoglu V, Ulker FD, Calıskan T (2008) "Smart structures and their applications on active vibration control: Studies in the Department of Aerospace Engineering. METU". Journal of Electroceramics 20(3-4), pp. 167-174.

[5] Sahin M, Aridogan MU (2011) Performance evaluation of piezoelectric sensor/actuator on active vibration control of a smart beam . Journal of Systems and Control Engineering Vol 225, 5, 533-547.

[6] Song G, Gu H (2007), Active Vibration Suppression of a Smart Flexible Beam Using a Sliding Mode Based Controller. Journal of Vibration and Control 13(8):1095-1107. DOI: 10.1177/1077546307078752

[7] Choi SB and Han YM (2010) Piezoelectric actuators: control applications of smart materials: CRC Press.

[8] Sivrioglu S, Tanaka N, Yuksek I (2002) Acoustic power suppression of a panel structure using H∞ output feedback control. Journal of Sound and Vibration 249(5) pp. 885-897.,

[9] Nestorovic T, Oveisi A (2015) Robust controller for the vibration suppression of an active piezoelectric beam. 7th ECCOMAS Thematic Conference on Smart Structures and Materials, Portugal, 3-6 June 2015 pp. 978-989.

[10] Sivrioglu S, Nonami K (1997) Active Vibration Control by Means of LMI-Based Mixed H2/H∞ State Feedback Control. JSME International Journal Series C 40(2):239-244.

[11] Zhou K, Doyle, JC (1999) Essentials of robust control: Prentice Hall.